Coupled Models of Lithospheric Flexure and Magma Chamber Pressurization at Large Volcanoes on Venus

Gerald A. Galgana[1*], Patrick J. McGovern[1], and Eric B. Grosfils[2]

[1]Lunar and Planetary Institute, USRA; [2]Geology Department, Pomona College
*Corresponding author, postal address: 3600 Bay Area Blvd., Houston, TX;
email: galgana@lpi.usra.edu

Abstract: We present an implementation of the Structural Mechanics module of COMSOL Multiphysics to model the state of stress associated with the emplacement of large volcanic edifices on the surface of a planet (in this paper, the planet Venus). These finite element models capture two essential physical processes: (1) Elastic flexure of the lithosphere (the mechanically strong outer layer of a planet) beneath the edifice load, and (2) Pressurization of a magma-filled chamber that serves as the supply source for the lava flows that build the edifice. We demonstrate that the COMSOL model adequately represents the response of an elastic plate to loading by benchmarking against an analytic axisymmetric flexure solution. We present results and preliminary interpretations of model stress states in terms of locations of predicted chamber wall failure and orientations of magma bodies (intrusions) emanating from the failed chamber.

Key words: Geomechanics, volcano-tectonics, crustal deformation, volcanoes, planetary science.

1. Introduction to Venus Volcano Morphology

The topography of the planet Venus is hidden beneath its thick and opaque atmosphere. Nonetheless, the Magellan spacecraft, equipped with Synthetic Aperture Radar (SAR), has imaged the surface of Venus at high resolution to reveal over 150 large volcanic edifices with lava flow diameters greater than 100 km [1, 2]. Identified on the basis of conical to domical topographic highs of several km and numerous digitate lava flows that form broad, flat aprons surrounding the edifices, these volcanoes are analogous to (but generally somewhat broader than) the gently sloped Hawaiian volcanoes on Earth.

For instance Sif Mons, a 2 km high by 200 km radius volcano on Venus, is characterized by gentle one to three degree slopes around the main edifice. These slopes evolve into lower slants of less than 1 degree on its outer flow apron [3].

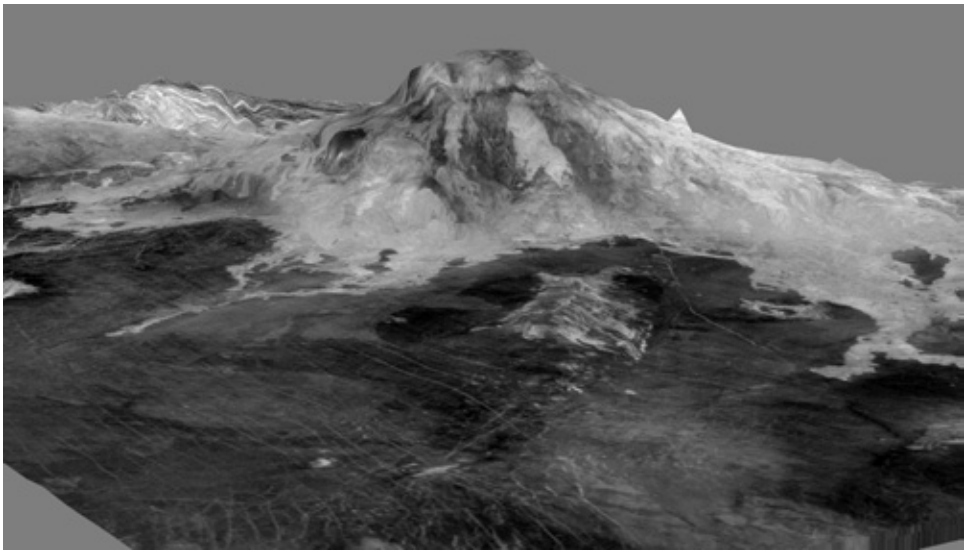

Figure 1. Perspective view of Maat Mons, the tallest volcano on Venus (height ~ 9 km above mean planetary radius). Synthetic Aperture Radar (SAR) backscatter image draped over DEM from altimeter. Vertical exaggeration is 25 x. Original data are from NASA's Magellan mission.

The main summit is dotted with calderae, radial pit chains, and fractures. Similarly, Maat Mons (Figure 1) features a significantly higher summit caldera, with the same broad, gentle slopes characterized by radial sheet and digitate lava flows. Both volcanoes, and many others like them, clearly add significant loads to the pre-edifice surface.

2. Theory of Volcanic Deformation and Elastic Flexure

Complementing field and analogue investigations, volcanic deformation on Earth has been explored in the past using analytical models. Inflating magma sources are commonly approximated as point, ellipsoidal, and crack-like sources of deformation, relating surface displacement to magma chamber pressure or volume change [i.e., 4, 5, and 6].

In addition, numerical finite element models provide the opportunity to explore further details, for instance by adding the effects of layering at various scales, varying reservoir geometry, or introducing the delayed pressure response caused by viscoelastic aureoles around terrestrial magma chambers [e.g.,7 – 13]. Use of numerical techniques is constantly evolving; as an example, elaborate models introduced recently include coupling of physical parameters such as thermal effects on strain [e.g., 14].

Both analytical and numerical approaches have been used to explore the effects of an overlying volcanic edifice load, and several authors have analyzed the resulting stress patterns around magma reservoirs and the implications for reservoir stability [e.g., 15, 16]. Recent models of magma chamber stability, which incorporate gravitational loading and lithostatic pre-stresses, have refined these efforts [e.g., 17], but until now interactions between magma chambers and flexural stress states have not been examined.

The loading effect of a volcanic edifice on the lithosphere can be considered as a flexing beam or plate problem in mechanics. The analytical flexure equation [18, 19], using a "thin-plate" approxi-mation that simplifies the mathematics, shows the relationship of a point load with the deflection of an elastic lithosphere (or alternatively, any loaded beam or plate):

$$D\frac{d^4w}{dx^4} = -(\rho_m - \rho_w)gw \qquad [1]$$

where w is the deflection, x is the distance from the loading point, D is the flexural rigidity, g is the gravitational constant (g = 8.87 m/s^2 for Venus), ρ_m and ρ_w are the density of the elastic lithosphere and the overlying mass. The amount of deflection throughout the section is described as a function of distance from the point of loading:

$$w(x) = \frac{V_o\alpha^3}{8D}e^{\frac{-x}{\alpha}}\left[\cos(x/\alpha) + \sin(x/\alpha)\right] \qquad [2]$$

where V_o is the load, and α is the flexural parameter. The flexural parameter (α) and the flexural rigidity (D) are described by the following equations:

$$\alpha = \left[\frac{4D}{g(\rho_m\rho_w)}\right]^{1/4} \qquad [3]$$

$$D = \frac{ET_e^3}{12(1-\upsilon^2)} \qquad [4]$$

Where T_e is the thickness of the elastic lithosphere, E is Young's Modulus, and υ is the Poisson's ratio.

More complete analytic models of plate flexure, the "thick-plate" formulations, account for shear and vertical normal stresses within the plate. We will use such a solution, the axisymmetric formulation of *Comer* [20], to benchmark our finite element solution (see below).

In a flexing lithosphere beneath the load, the upper part experiences horizontal compression while the lower part experiences horizontal extension: a "dipole" state of stress. The central part is a low-stress/strain region called the neutral plane. The maximum deflection occurs at the point near the load, which steadily decreases towards the hinge line (termed the forebulge, which is a topographic high), a distance from the point of loading. The distant section of the lithosphere experiences negligible deformation.

3. Method

We implement a series of numerical experiments with the COMSOL Multiphysics Structural Mechanics Module [21], in order to evaluate how a flexural stress state changes the characteristic response of a pressurized, inflating magma chamber. We consider variations in both the lithospheric stress state (modulated by elastic lithosphere thickness T_e and volcanic load magnitude) and magma chamber stresses (controlled by chamber radius, magma density and overpressure). The depth at which the chamber is embedded in the lithosphere is a critical parameter, as it affects the characteristic stress state (horizontal extension or compression) encountered by the chamber.

We use the COMSOL Structural Mechanics Module to build a two-dimensional axisymmetric elastic model of the Venusian lithosphere, loaded with a large, conical volcanic edifice of radius 200 km and height 5 km (Figure 2). This volcano is situated at the center of a model domain extending out to 900 km. We adopt two elastic lithosphere thicknesses (i.e., T_e = of 20 and 40 km), representing the best estimates of elastic thickness of the Venusian lithosphere. This is consistent with values derived from topographic profiles and topography/gravitational admittance models for Venus [22, 23]. The material parameters of the lithosphere and the volcano correspond to those adopted by *McGovern and Solomon* [2].

The effects of gravitational loading are added to the model through body forces, including "lithostatic" pre-stress. The response of the asthenosphere (or the mechanically weak, viscously deforming zone beneath the lithosphere) is modeled as a buoyant fluid with "Winkler"-type restoring forces applied to the base of the model. A constant force counteracting the vertical pre-stress is also applied at the base. The volcano edifice in each model acts as a distributed load on the surface, and bends the lithosphere. Vertical roller conditions are applied at the outer boundary of the model to constrain horizontal motions at that end.

A pressurized spherical magma chamber is emplaced at the center of each coupled model; emplacement depth and diameter are varied. We use radii of 1 km for the small magma chamber and 3 km for the large magma chamber. We prescribe an overpressure (simulating inflation) on the wall of the magma chamber to the point where maximum stresses reach the critical fracture point, assumed here as the onset of tensile (or positive) stress values.

Using these parameters, COMSOL solves for stresses in and deformation of the lithosphere, including stresses along the magma chamber wall. From the results, we examine the stress distribution of the lithosphere, and determine the relationship of flexure and reservoir pressurization.

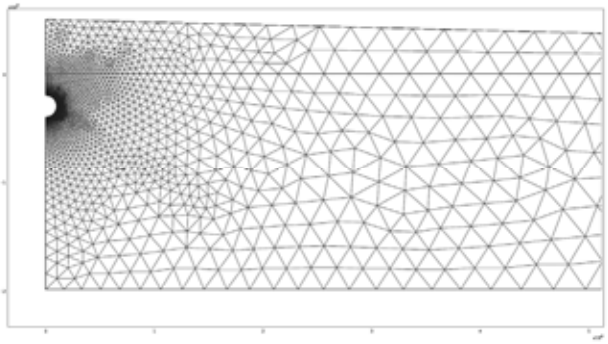

Figure 2. A close-up of a portion of the finite element mesh near the symmetry axis, for the thin lithosphere model with a three-kilometer deep magma chamber. This model comprises about 17,100 triangular elements. The spatial resolution of individual elements increases toward the curved magma chamber.

4. Benchmark

To demonstrate the ability of COMSOL Multiphysics to model flexure, we benchmark a simplified model (lacking a structural edifice and magma chamber) to the analytic thick-plate axisymmetric flexure solution of *Comer* [20].

In the COMSOL benchmark model, the load of the edifice is represented as a sum of point loads applied to the surface of the plate, rather than as a stress-bearing mechanical extension of the model domain as in the full coupled models. This ensures an "apples-to-apples" comparison with the analytic models, in which the edifice load is also not stress-bearing.

In the benchmark model, the load is equivalent to that exerted by a 4 km high by 200 km radius volcano on Venus, slightly smaller than our final models with magma chambers. The COMSOL model matches the surface displacement of the analytic solution very well (Figure 3). With this positive correlation, we run several models with magma reservoirs and varied lithosphere thicknesses, and observe the correlations between stresses and flexure.

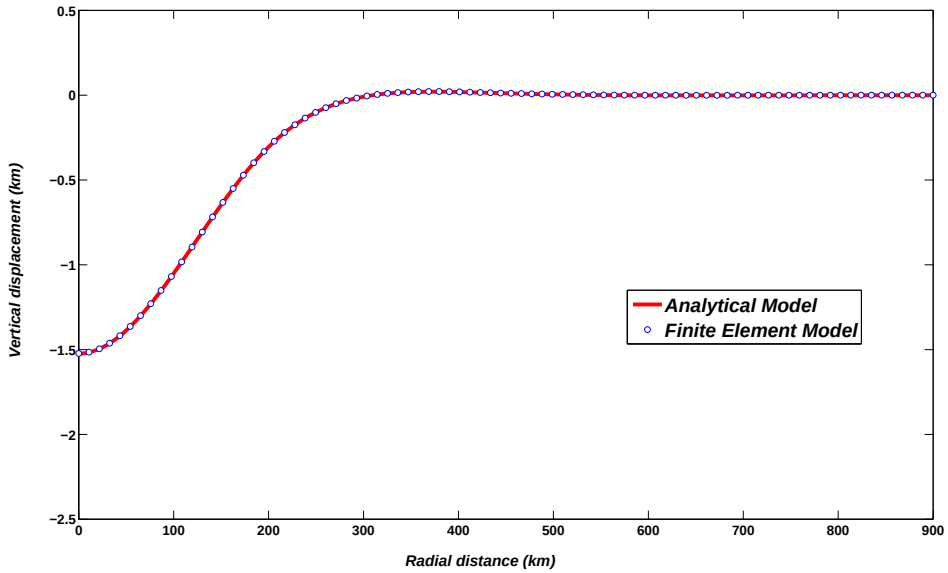

Figure 3. Topography after loading (T_e = 40 km, the vertical exaggeration is ~ 200:1). The finite element model is 99.9% accurate compared with the analytical solution.

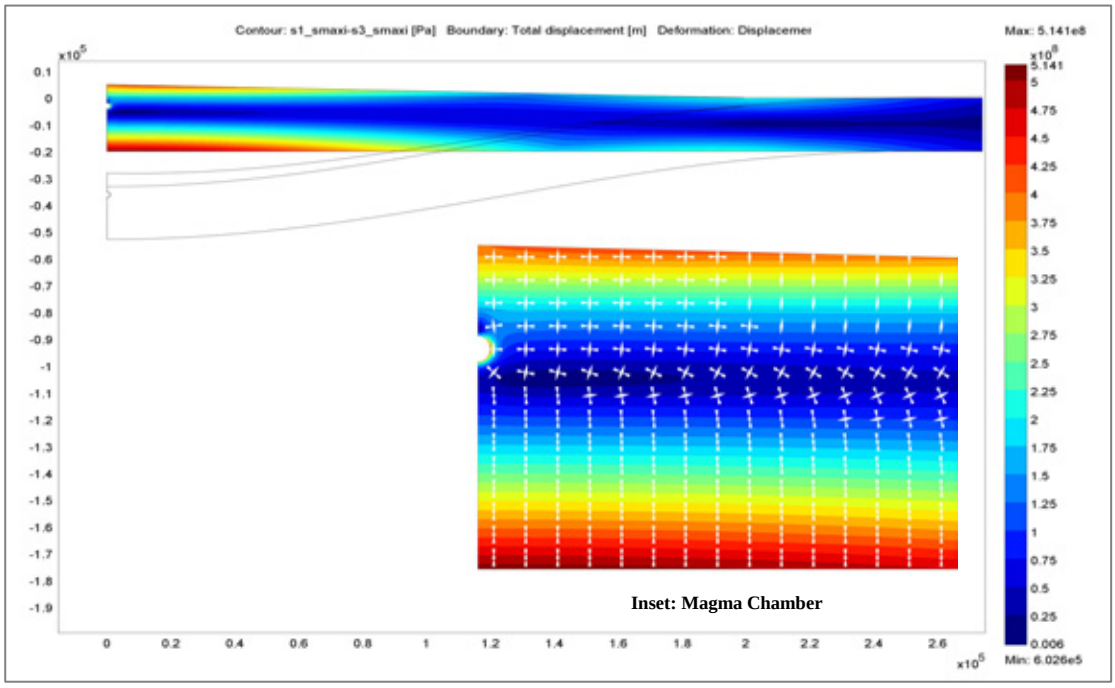

Figure 4. Axisymmetric model of the lithosphere showing differential stresses (T_e = 20 km, red = high differential stresses; blue = low differential stresses), and flexural deformation after loading. A small (r = 1 km), spherical magma chamber is located at the left side, 3 km deep at the axis of symmetry. Outline shows deformed lithosphere after loading (deformations exaggerated by a factor of 10). This image is a subset of the 900-kilometer radius axisymmetric model. Inset shows zoom of region with the overpressured magma chamber; Colors show differential stresses, while arrows depict principal stress directions.

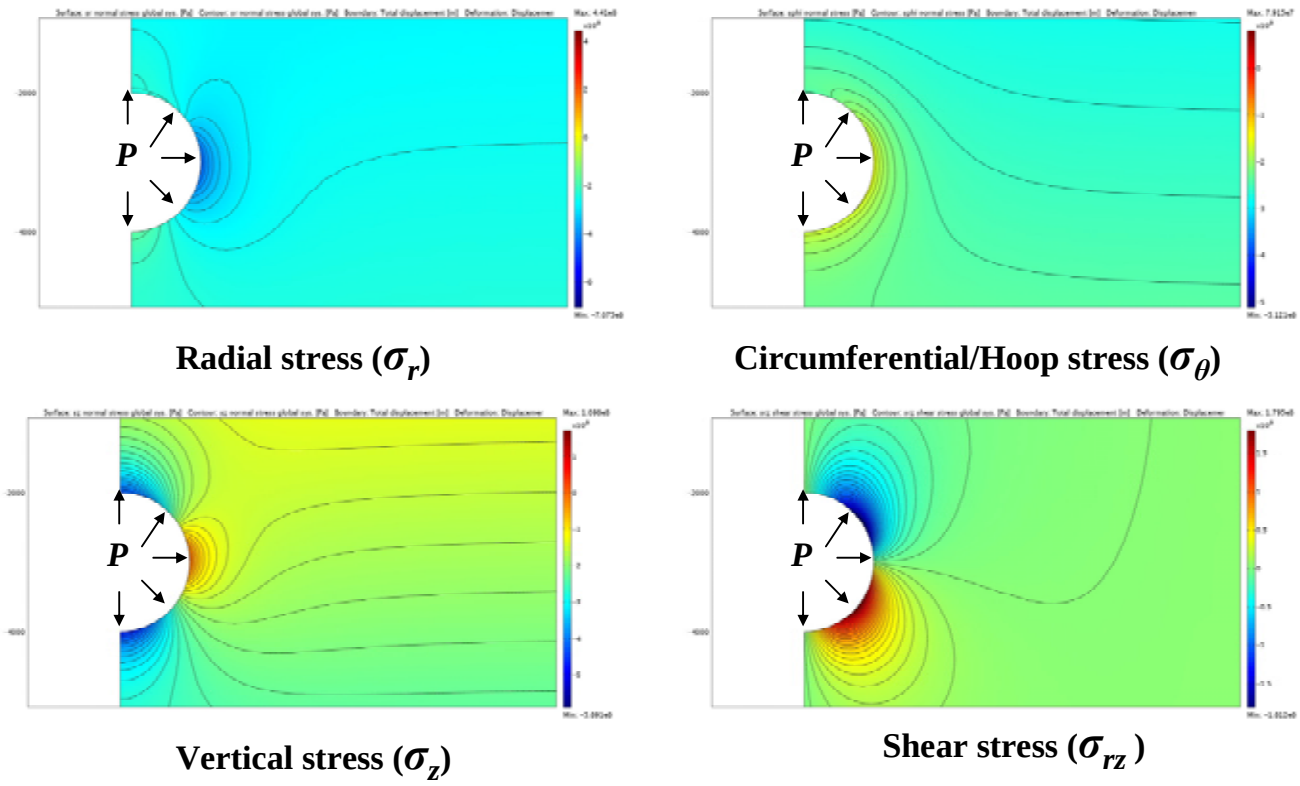

Figure 5. Model results showing stress components around the spherical magma chamber, for the thin lithosphere model (Red = extension, Blue = compression); *P* is the critical pressure at which the reservoir will rupture, with simple overpressure and magma weight combined.

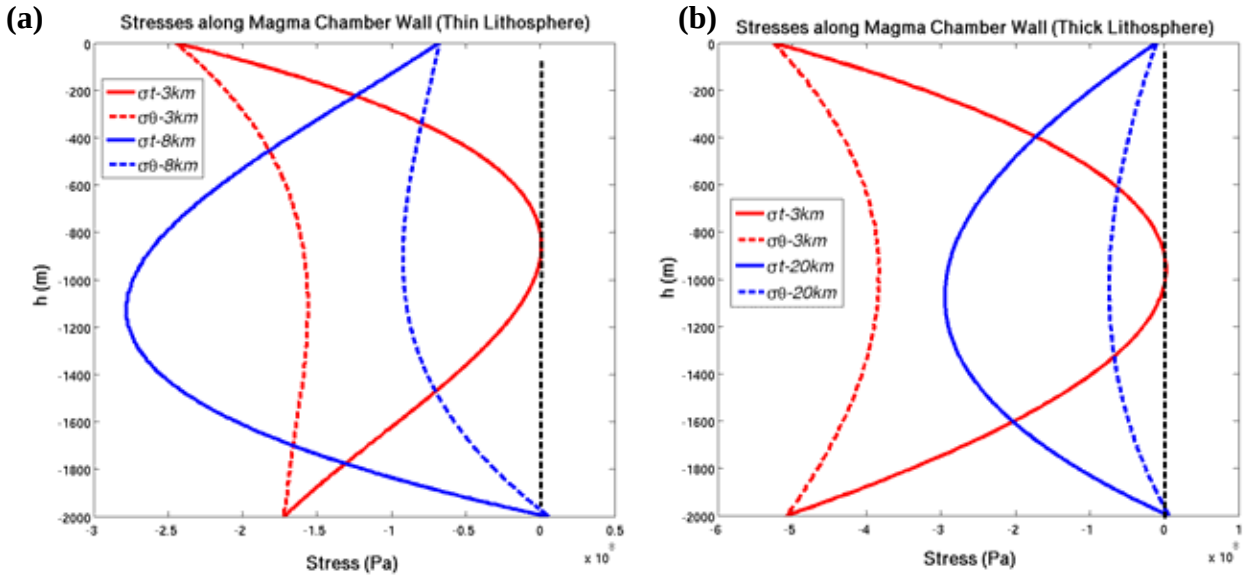

Figure 6: Tangential (σ_t) and hoop (σ_θ) stresses along magma chamber wall, for 3 km- and 8 km- deep spherical reservoirs of radius 1 km embedded in a 20 km-thick lithosphere (***Figure 6a, left figure***). ***Figure 6b*** (***right***) plots the stresses for the 3 km- and 20 km-deep reservoirs within a 40-km thick lithosphere. Stress (x 10^8 Pa) is measured on the x-axis, with negative values showing compression. Dashed vertical black line indicates the start of the failure zone. The y-axis shows vertical depth within the magma chamber; crest is zero, while the bottom is -2000 m. Maximum tensile stresses, showing areas of possible failure, occur near the center of the 3-km deep reservoirs but near the bottom of the 8-km deep reservoir.

5. Results and Discussion

After loading, our models predict a flexural stress state consistent with deflection patterns shown by analytic equations. Towards the model center, high differential stresses exist on the upper and lower parts of the lithosphere, separated by a region of low stresses along the central neutral plane. Horizontal stresses in the upper lithosphere are predominantly compressional, complemented by extensional stresses in the lower lithosphere (Figure 4). Low stresses are found at the outer regions of the models.

Significantly high stresses are found near the magma chamber wall, which rapidly decreases as a function of radial distance from the center (Figure 5). The curves in Figure 6 show horizontal stresses after pressurization at the margin of the magma chamber: out-of-plane stress σ_θ (dashed) and wall-parallel stress σ_t (solid). Failure of the reservoir occurs where stresses approach tensile values (tensile strengths of basaltic materials are generally 10 MPa or less). For a chamber situated in the lower lithosphere (blue curves), the highest stress is predicted at the bottom of the chamber. In contrast, for a chamber emplaced in the upper lithosphere (red curves), the zone with the highest stress is near the center of the chamber.

6. Conclusions

We demonstrate that combined reservoir pressurization and flexural stresses can be implemented effectively using the Structural Mechanics module of COMSOL Multiphysics. The stresses and deformation resulting from our models outline the expected patterns within the lithosphere after volcano edifice loading. This approach can be used in analyzing crustal deformation where large volcanoes are involved, such as those situated on Venus and Mars. Model results can be used to study patterns of magma reservoir failure, including patterns of magma intrusion and propagation, assess eruption potential, and understand the long-term process of volcano evolution.

7. References

1. Crumpler L., et al., Volcanoes and Centers of Volcanism on Venus. In Bougher, Hunt, and Phillips (eds.), *Venus II: Geology, Geophysics, Atmosphere and Solar Wind Environment*, University of Arizona Press, Tucson AZ (1997).

2. McGovern, P. J., and S. C. Solomon, Growth of large volcanoes on Venus: Mechanical models and implications for structural evolution. *Journal of Geophysical Research*, 92, 103(E5):11,071-11,101 (1998).

3. Stofan, E., J. Guest, and D. Copp, Development of Large Volcanoes on Venus: Constraints from Sif, Gula, and Kunapipi Montes, Icarus,, 152:75-95 (2001).

4. Mogi, K., Relations between the eruptions of various volcanoes and the deformations of the ground surfaces around them, *Bulletin Of the Earthquake Research Institute*, 36: 99-134 (1958).

5. Davis, P.M., Surface deformation due to inflation of an arbitrarily oriented triaxial ellipsoid cavity in an elastic half-space, with reference to Kilauea volcano, Hawaii, *Journal of Geophysical Research,* 80: 4,094-4,102 (1986).

6. McTigue, D.F., Elastic stress and deformation near a finite spherical magma body: resolution of the point source paradox, *Journal of Geophysical Research,* 92: 12,931-12,940, (1987).

7. Dieterich, J. and R. Decker, Finite Element Modeling of Surface Deformation Associated with Volcanism. *Journal of Geophysical Research*, 80 (29): 4,094-4,102 (1975).

8. Trasatti, E., C. Giunchi, M. Bonafede. 2003. Effects of topography and rheological layering on ground deformation in volcanic regions. *Journal of Volcanology and Geothermal Research,* 122: 89-110.

9. Newman, A., T. Dixon, G. Ofoegbu, and J. Dixon, Geodetic and seismic constraints on recent activity at Long Valley Caldera, California: evidence for viscoelastic rheology, *Journal of Volcanology and Geothermal Research,* 105: 183-206 (2001).

10. Manconi, A., T. Walter, and F. Amelung, Effects of mechanical layering on volcano deformation, *Geophyical. Journal International,* 170 (6807):952-958 (2007).

11. Masterlark, T., Magma intrusion and deformation predictions: Sensitivities to the

Mogi assumptions, *Journal of Geophysical Research* ,112(B6): B06419 (2007).

12. Grosfils, E., Magma reservoir failure on the terrestrial planets: Assessing the importance of gravitational loading in simple elastic models. *Journal of Volcanology and Geothermal Research*, 166: 47-75 (2007).

13. Long, S.M., and E.B. Grosfils, Modeling the effect of layered volcanic material on magma reservoir failure and associated deformation, *Journal of Volcanology and Geothermal Research* 186: 349-360 (2009).

14. Del Negro, C., G. Currenti, and D. Scandura, Temperature-dependent viscoelastic modeling of ground deformation: application to Etna volcano during the 1993-1997 inflation period, *Physics of Earth and Planetary. Interiors*., 172: 299-309 (2009).

15. Sartoris, G., J. Pozzi, C. Philippe, and J. Le Moüel, Mechanical stability of shallow Magma Chambers, *Journal of Geophysical Research*, 95(B4): 5141-5151 (1990).

16. Pinel, V. and C. Jaupart, Magma chamber behavior beneath a volcanic edifice. *Journal of Geophysical Research*, 108(B2): 2072 (2003).

17. Hurwitz, D.M., S.M. Long, E.B. Grosfils, and P.J. McGovern, A revised simple elastic model of magma reservoir failure beneath a volcanic edifice, *Proceedings of the Lunar and Planetary Science Conference 2009*, Houston, TX (Abstract #1220) (2007).

18. Timoshenko, S., Strength of Materials, Part II: Advanced theory and problems: New York, D. Van Nostrand Co. 572 pp. (1958).

19. Walcott, R., Flexural rigidity, thickness, and viscosity of the lithosphere. *Journal of Geophysical Research*, 75:3941-3953 (1970).

20. Comer, R.P., Thick Plate Flexure. *Geophysical Journal of the Royal Astronomical Society*, 72:101-113 (1983).

21. COMSOL AB, *Comsol Multiphysics Reference Manual*, Version 3.5, Stockholm, Sweden, 2008.

22. Phillips, R. et al., 1997. Lithospheric Mechanics and Dynamics of Venus, In S. Bougher, D. Hunten, and R. Phillips (eds.), *Venus II: Geology, Geophysics, Atmosphere and Solar Wind Environment*, Univ. Arizona Press.

23. Simons, M., S. C. Solomon, and B. H. Hager, 1997, Localization of gravity and topography: constraints on the tectonics and mantle dynamics of Venus, *Geophys. J. Int., 131*, 24-44.

8. Acknowledgments

This research was funded by NASA Planetary Geology and Geophysics grants, and by the Lunar and Planetary Institute. LPI Contribution # 1513.